Original Research

A new neurotoxicity model composed of a neurovascular unit in vitro

C. Wang, W. Gu, K. Zhao, H. Zhang, Y. Li, X. Bai[*]

Insititute of Environmental Health and Related-Product Safety of the Chinese Center for Disease Control and Prevention, Beijing 100021, China

Abstract: In this study, we established a 2-D model composed of brain microvascular endothelial cells (BMECs) and neurons, and a new 3-D model called a neurovascular unit (NVU) that included co-culturing with BMECs, hippocampal neurons, and astrocytes. First, three different cell types (BMECs, hippocampal neurons, and astrocytes) were cultured and identified; then, positive neurotoxic chemicals were used to test cell viability. Half maximal (50%) inhibitory concentration (IC50) and intracellular calcium concentrations were calculated using primary cells in both models. The results showed that Pb^{2+} and AL^{3+} exposure significantly decreased cell viability and increased intracellular calcium concentrations. The two experimental models did not display any differences in cell viability and intracellular calcium concentrations compared to the control, but they did show declining cell viability with increasing Pb^{2+} and AL^{3+} concentrations. The permeability results suggested Pb^{2+} and AL^{3+} could change the permeability of the two models. In conclusion, the two models replicated the blood-brain barrier (BBB) more accurately than the control, so it has potential usefulness in further scientific and clinical drug research. Furthermore, NVU model could be used to screen neurotoxicity chemicals due to its NVU properties.

Key words: Neurovascular unit (NVU), Cell morphology, cell viability, GFAP, MAP2, Factor–VIII, immunohistochemical, immunofluoresce, intracellularCa²⁺, Permeability.

Introduction

The BBB is an active interface that restricts free substance movement between the circulatory and central nervous systems (CNS); it plays a key role in maintaining CNS homeostasis (1). Establishing a BBB model is critical for developing drugs and evaluating chemical neurotoxicity. BBB models were originally based on non-cerebral cells in vitro. As a result, the scientific community has advanced models based on a co-culture with cerebral endothelial cells.

Researchers have recognized that brain health involves complex functional interactions between neurons and non-neuronal cells (2,3); recently, the concept of the NVU has been developed. The nerve vascular unit which consists of endothelial cells, pericytes, microglial cells, and neurons, couples local neuronal functions to local cerebral blood flows and regulates blood-borne molecule transportation across the BBB (4). The vascular system

provides glucose, oxygen, and hormones for brain cells and guides the cells to respond to the local environment; the brain also regulates blood vessels in responses to local requirements. Non-neuronal cells chargephysical, biochemical, and immune CNS barriers, which regulate signal transduction, remodeling, angiogenesis, and neurogenesis. Tri-culture models with endothelial cells seeded on a transwell membrane, astrocytes seeded on the opposite side of the membrane, and the neurons or pericytesseeded on the bottom of the culture dish have been found to improve BBB properties compared with the co-culture model (5, 6).

The vitro BBB model is characterized by cell morphology and expression of specific markers and functions. We evaluated the two models with the accepted evaluation system. This study explored the viability of a new model, NVU, which could potentially replace BBB models as an investigative tool for neurotoxic chemicals and their mechanisms. We established two models: one was composed of brain microvascular endothelial cells (BMECs) and neurons; the other included co-culturing with BMECs, hippocampal neurons, and astrocytes.

In this study, we cultured astrocytes, BMECs, established monolayer BMECs, hippocampal neurons, and a tri-cultivation Transwell model, which used hippocampal neurons as experimental points. The experimental results indicated that we successfully established these factors. The data also revealed potential neurotoxic chemical mechanisms.

Materials and Methods

Animals

Newborn Wistar rats were purchased from the Laboratory Animal Center of Academy of Military Medical Sciences (Beijing, China). Postnatal rats were humanely euthanized following approved guidelines.

Chemicals

Poly-L-Lysine (MW: 30, 000-70, 000), Insulin, Collagenase,Cytosine arabinoside, and L-Glutamine (200mM) were purchased from Sigma-Aldrich (St Louis, MO, USA). Horse serum, Fetal Bovine Serum, B-27® Serum-Free Supplement (50X), antibiotic antimitotic (100X), DMEM (High Glucose), HBSS (10X), HEPES (1M), Trypsin (1: 250), and Neurobasal®-A

Medium (1X) were purchased from Invitrogen (California, USA). The purchased antibodies were from a Santa Cruz company (Texas, USA).Resazurin was obtained from Alfa Aesar (Ward Hill, MA, USA). Sodium fluorescein and the Fura-2/AM kit was purchased from Dojindo (Japan). Pb $(CH_3COO)_2 \cdot 3H_2O$ and $Al_2(SO4)_3.18H_2O$ were purchased from Sinopharm Chemical Reagent Co., Ltd.

Isolation and culture of primary astorcyts, BMECs, and hippocampal neurons

First, we removed the rat skulls and dissected the hippocampus and cortex using a pair of fine tweezers. We then placed the specimens into separate 6-cm diameter culture dishes with cold HBSS (1X). We removed the cerebral hemispheres and carefully stripped away the tissue with fine forceps. Finally, we washed the tissue with cold HBSS(1X) twice and cut it into 1mm^3 pieces.

For astrocytes (As) culture, cerebral astrocytes were performed as described above, with the following changes (7). The cortical pieces were digested in trypsin (1.25mg/ml) at 37 °C for 5 min. The cell suspension was filtered through a 70µm cell strainer. After being centrifuged at 100(×g) for 5 min, the precipitate was re-suspended with a DMEM (high glucose) culture medium (including 10% FBS, penicillin(100.0 U/ml), streptomycin(100.0mg/ml)) and cultured with 25cm^2 plastic dishes pre-coated with Poly-L-Lysine (0.1mg/mol) at 37 °C and 5% CO2. On the fourth day, we stroked the dishes several times to remove the upper adherent cells. The cells were further purified by a trypsin (2.5% mg/ml) solution when the cells reached 80% confluence.

For BMECs culture, the primary BMECs were processed according to Diglio's method (8). The brain cortex pieces were homogenized with a glass homogenizer. In turn, the suspension was filtered through a 70µm and 100µm cell strainer. After being centrifuged at 400(×g) for 20 min, the homogenized mixture were digested at 37 °C for 7 min by collagenase type II (1mg/ml). Then, it was warmed in a DMEM medium and 10% FBS was added to stop digestion. The suspension was centrifuged at 200(×g) for 10 min. We then resuspended the cells in a DMEM (high glucose) medium (consisting of 15% FBS, 20% FBS, basic fibroblast growth factor (bFGF, 150µg/ml), heparin (120U/ml), L-Glutamine (2mM), Gentalline (100U)). BMECs were seeded on 25cm^2 dishes which waspre-coated with Poly-L-Lysine (0.1mg/ml) and incubated at 37 °C. The endothelial cells were further purified with collagenase type II (1mg/ml) when the confluence reached 80% on the 7th day.

For cerebral hippocampal neurons culture, rat cerebral hippocampal neurons were processed according to previous research (9). The cortex pieces were digested with trypsin (1.25 mg/ml) at 37 °C for 7 min. Then, we transferred the supernatant to a 6-cm culture dish and added a neuronal plating medium (composed of DMEM with 10% Horse serum, penicillin (100 U/ml), streptomycin (100µg/ml)). The chunks were gently aspirated with a 1 ml pipette 10 times, and then left to settle for a few minutes. Then, the suspension was filtered through a 70µm cell strainer. The precipitate was further re-suspended with DMEM (10% horse serum and seeded on plates or plastic culture flask pre-coated with poly-L-ly-

sine (0.1 mg/ml)) at 37 °C and 5% CO2. On the second day, medium was replaced by a neuronal maintenance medium (Neurobasal®-A Medium (1X), containing B27 (1×), penicillin (100.0 U/ml), streptomycin (100ug/ml)). On the third day, medium was replaced by a new medium supplemented with Ara-C (5.0µM) to inhibit non-neuronal cell growth.

Establishing a 2-D and NVU model

The two models require high BMECs and astrocytes cell purity. In the 2-D model, BMECs (1.5x10^{5}cells/ml) were seeded on the inner side of the transwell membrane (Millipore Plate Insert); NVU model was prepared according to Schiera's method(10). Astrocytes (5×10^{5}cells/ml) were planted on the outer side of the Transwell membrane for 1 day, and then the Transwell was converted on the 24 well culture plate and left to culture for 3 days until reaching 70% confluence. BMECs were planted in the inner side of the inset membrane until reaching 90% confluence.

Immunofluorescence assay

Different cells were characterized by specific markers according to a previous study (11). Cells were obtained from previous cultivations and fixed with 4% paraformaldehyde for 30 min at 4 °C. After removing excessive paraformaldehyde, cells were incubated in 0.5% Tritonx-100 for 10 min, and a blocking serum (3% BSA with 0.5% Tritonx-100) for 30 min at room temperature. Then, cells were washed with PBS 3 times after incubation; the blocking serum was not washed. BMECs and astrocytes cells were incubated with primary antibodies (anti-glial fibrillary acidic protein (GFAP) for astrocytes; anti-factor VIII for BMECs) overnight at 4 °C (1:200 dilution). Cells were then incubated with FITC- chicken anti-rabbit- IgG (1:100) and chicken TR -anti-goat IgG (1:100) in PBS containing 3% bovine serum albumin and 0.5% Tritonx-100. Finally, cells were observed through a fluorescence microscope (OLYMPUS, Japan).

Immunocytochemical staining

MAP2 was chosen as a specific marker for hippocampal neuron identification. The beginning steps were the same as those of the BMECs and astrocytes. The cells were covered overnight with primary antibody anti-MAP2 at 4 °C, which was diluted 1:20 in PBS with 3% bovine serum albumin and 0.5% Tritonx-100. On the second day, we washed the cells with PBS and incubated them with horseradish peroxidase (HRP) -goat anti-rabbit IgG (1:100) in PBS containing 3% bovine serum albumin and 0.5% Tritonx-100. We added a DAB kit for 5 min and washed the DAB with water until the color was perfect. Cell were observed through an inverted microscope (OLYMPUS, Japan).

Assaying cell viability

The separately cultured cells including astrocytes, BMECs, and hippocampal neurons were seeded in the 24-well plates and treated for 3h. We chose the below concentrations based on the pre-test results:Pb^{2+} concentrations were 25µmol/L, 50µmol/L, 100µmol/L, 200µmol/L, 400µmol/L, 800µmol/L, 1600µmol/L, and3200µmol/L; Al^{3+} concentrations were 125µmol/L,

250μmol/L, 400μmol/L, 500μmol/L, 800μmol/L, 1000μmol/L, 1600μmol/L,2000μmol/L, 2400μmol/L, 4000μmol/L. Each group had two parallels. The two type cell model concentrations were as follows: Pb^{2+} concentrations were 50μmol/L, 100μmol/L, 200μmol/L, 400μmol/L, 800μmol/L, 1600μmol/L, and 3200μmol/L; Al^{3+} concentrations were 62.5μmol/L, 125μmol/L, 250μmol/L, 500μmol/L, 1000μmol/L, and 2000μmol/L. After 3h of cultivation, the cells were washed with HBSS and an Alamar-Blue detection reagent (5μmol/L) was introduced for a 4h cultivation period. Fluorescence was measured using a TECAN GENIOS(Thermo Fisher scientific, USA) with a 530 nm excitation wavelength and 590 nm emission wavelength.

Measuring Transendothelial Electron Resistance (TEER)

The 2-D and NVU models were prepared as above. When the cells reached 95% confluence, the transendothelial electrical resistance (TEER) was measured using a MILLICELL-ERS (Millipore, Billerica, MA) according to the manufacturer's instructions. The two electrodes were placed in the lower and upper dual chamber system compartments. The TEER was measured every hour for 5 times at room temperature. It has been demonstrated that above 120-130 $Ohmxcm^2$ TEER values, sodium fluorescein and FITC-labeled dextrane (4kDa) permeability does not decrease as TEER increases (12), indicating that barriers with at least 120-130 $Ohmxcm^2$ can be used for transport experiments (13).

Permeability measurements

The barrier function can be evaluated by measuring cell permeability. Sodium fluorescein (MW=376 Da) is used as tracer. The apparent permeability is determined using the following formula: $Papp = Dq/(dTxAxC_0)$, where dQ is the transported amount, Dt is the incubation time, A is filter surface, and C_0 is the initial concentration. Permeability values in the order of magnitude of 10^{-6}cm/s for sodium fluorescein were considered good values (14,15,16). We designed the control group and test groups; each group had three parallel samples. We chose sodium fluorescein as the tracer and removed the same amount of liquid at different times. The TECAN GENIOS determined that the excitation wavelength was 428nm and the emission wavelength was 536nm. Finally, we calculated Pe according to the formula.

Determination of intracellular calcium

Primary cells and cell models were prepared through the above methods. The astrocytes, BMECs, and hippocampal neurons of the two models were treated with different Pb^{2+} concentrations (50μmol/L, 100μmol/L, 125μmol/L, 150μmol/L, 200μmol/L, 250μmol/L, 500μmol/L, and 1000μmol/L) for 3h; the control was the culture mediumAl^{3+} (62.5μmol/L, 125μmol/L, 200μmol/L, 250μmol/L, 400μmol/L, 500μmol/L, 600μmol/L, 800μmol/L, 1000μmol/L). After removing treated medium, cells were washed with HBSS 3 times. A Fura - 2 / AM working liquid (5 μmol/L) was added, and the cells were incubated for 20 min at 37 °C. Then, we removed the Fura - 2 / AM working liquid and washed the cells with HBSS 3 times, finally adding HBSS that contained calcium and magnesium; they were incubated for 20 min at 37 °C to process the esterification. The results were measured with a TECAN GENIOS under a 380 nm excitation wavelength and 510 nm emission wavelength. The calculation formula is as follows: intracellular free Ca^{2+} concentration = Kd (F0 / FS) (R - Rmin)/(Rmax - R). The Kd value is 224 nmol/l; F0 and FS represent the measured Ca^{2+} fluorescence intensity at a zero saturation state, R is for the observed fluorescence ratio, and Rmin and Rmax are the maximum and minimum fluorescence ratio, respectively.

Results

Cell morphology of astrocytes, BMECs, hippocampal neurons, mono-culture BMECs, and tri-culture BMECs co-cultured with astrocytes

Primary cells were prepared according to the above methods. Cells originally attached to the bottom of the culture dishes like spheres. After three subculture passes, the cells were separated and grew into single cells (Fig. 1A). They were digested with trypsin (1.25mg/ml); microvascular endothelial cells presented a string of beads. After a 4h culture, microvascular endothelial cells attached to the bottoms of dishes. During the culture, cells grown from the cell fragments mixed with other cells like neurons (Fig. 1 B). After three subculture passages, the cells were mostly BMECS because they were cultured with a specialized medium that purifies BMECs. Hippocampal neurons attached to the dish walls after 4h. 48h after Ara-C (5.0μmol/L) was added, most cells were hippocampal neurons. On the fifth day, networks formed between the cells and synapses (Fig. 1C). Hippocampal neurons survived for about 3 weeks.
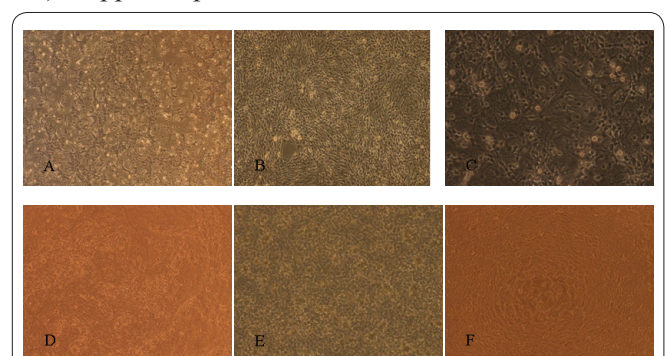
Figure 1. Cell morphology of astrocytes, BMECs, hippocampal neurons, and the two NVU models. After two subculture passages, the composition was complicated and mixed with other cells, such as neurons or fiber cells. The astrocytes were irregular in shape and had abundant cytoplasm. After three culture passages, the astrocytes exhibited signals (1A, X40). Primary cultured BMECs were polygonal or shaped like a long spindle, and resembled paved stone (1B, 100X). Primary cultured hippocampal neurons were shaped like triangles, spindles, or had an irregular shape. On the fifth day, the number of synapses increased, interaction connections between cells were complex, and they formed a very dense network. The cell body was strongly reflected and nuclei were yellow (1C, 200X). The BMECs were cultured in the insert membrane for 5 days (1D, 100x) and cells reached 80% confluence. Atrocyte cells were seeded on the bottom of the insert membrane for 3 days (1E, 100X) and cells reached 80% confluence. Two sides of the insert membrane were planted with astrocytes and BMECs (1F, 100X) and formed a more dense network.

Mono-culture BMECs were planted in the insert membrane and cultured until confluent (Fig. 1D). The tri-culture BMECs co-cultured with astrocytes on the outer and inner side of the insert membrane grew until reaching 90% confluence. Cell morphology was observed through an inverted microscope (Figs. 1E, 1F).

Identifying astrocytes, BMECs, and hippocampal neurons

According to the previous primary culture method, the cells were seeded on glass cover slips coated with Poly-L-Lysine. Astrocytes and BMECs were labeled with FITC and TR. Astrocytes expressed glia fibrillary acidic protein (GFAP), the cytoplasm presented green (Fig. 2A), nuclei were round or oval, and thenucleoli were not in the middle; BMECs expressed F-VIII related antigen, cytoplasm showed red fluorescence, nuclei had multiple shapes (Fig. 2B), hippocampal neurons expressed MAP-2 antigen, and cytoplasm and axons showed yellow fluorescence using horseradish peroxidase as a labeled antibody (Fig. 2C). The 2-D and 3-D models were prepared under the preceding method. They also each respectively showed red or green fluorescence through a fluorescence microscope (Figs. 2D & 2E).

Cell viability assay

When treated with Pb^{2+} and Al^{3+}, cell viability of astrocytes, BMECs, and hippocampal neurons were significantly reduced compared with the control group
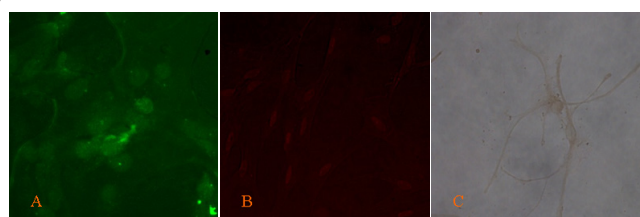
Figure 2. *Identifying astrocytes, BMECs, and hippocampal neurons.*Astrocyte cytoplasm was green and nuclei were round or oval when observed by fluorescence microscope labeled by FITC, which expressed GFAP (2A, 200X). BMEC cytoplasm and nuclei were red when observed by a fluorescence microscope labeled by TR, which expressed F-VIII related antigen (2B, 200X). Hippocampal neuron cytoplasm and axons were brown when observed through an inverted microscope labeled by Horseradish peroxidase, which expressed MAP-2 (2C, 400X).
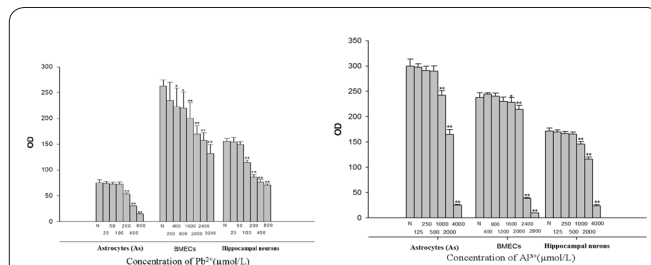
Figure 3. OD Value of astrocytes, BMECs, and hippocampal neurons with different Pb^{2+} and Al^{3+} concentrations. P<0.01compared with control.
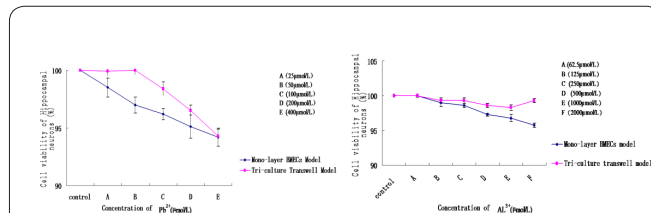
Figure 4. Cell viability for different treatments and concentrations on 24-well plates. The two models did not display any significant differences in cell viability compared with the control; they decreased with the concentration.

(Fig. 3). However, hippocampal neuron viability in the mono-layer BMECs model and tri-culture Transwell model did not show significant differences compared with the control group (Fig. 4). Table 1 shows the IC50 of the three primary cultured cells types.

Measuring Transendothelial Electron Resistance (TEER)

We measured the TEER value before and 3h after Pb^{2+} and Al^{3+} treatment for the two models. The results showed that both the 2-D and 3-D models had significant differences between the pre- and post-test. TEER values were above $130\Omega xcm^2$ before the test, and suitable for further study.

Four hours leakage detection assay

The liquid level for the chosen 2-D and 3-D models displayed no difference between the donor pool and pools before and after 4h of incubation. Models that did not follow this trend were abandoned.

Permeability measurements

The results are shown in table 2.

Table 1. IC50 for astrocytes, BMECs, and hippocampal neurons treated with Pb^{2+} and Al^{3+} ($\overline{x}$±s, n=4).

IC50	AS	BMECs	Hippocampal neurons
Pb^{2+}	250.1±17.9	3245.1 ±100.3	226.7±14.3
Al^{3+}	2481.1±558.3	2668.8±36.1	2129.1±228.3

IC50 for astrocytes, BMECs and hippocampal neurons. The IC50 of astrocytes and hippocampal neurons were different from those of BMECs. Pb^{2+} and Al^{3+} toxicity on the three cell types were different because of different sensitivity with different chemical materials or perspective cell characteristics.

Table 2. Permeability for the 2-D and 3-D models treated with Pb^{2+} and Al^{3+}, respectively ($\overline{x}$±s, n=3)

Pe (x10⁻³ cm/min)	control	Pb^{2+}	Al^{3+}
2-D model	1.02±0.09	3.07±0.27	2.98±0.08
3-D model	1.02±0.09	2.58±0.43	2.38 ±0.29

We calculated the fluorescence intensity (FI) of the medium, which had sodium florescein at 10, 20, 30, 40, 50, and 60 min. We then calculated the permeability coefficient (Pe).

Intracellular calcium assay

Primary astrocytes, BMECs, cerebral hippocampal neurons, and 2-D and 3-D models were treated with different Pb^{2+} and Al^{3+} concentrations for 3h. The intracellular Ca^{2+} concentration was measured by TECAN GENIOS. Fig. 5 shows the intracellular Ca^{2+} concentrations of astrocytes, BMECs, and hippocampal neurons. The results showed that the intracellular Ca^{2+} concentrations of all three cell types increased after Pb^{2+} and Al^{3+} incubation (Fig. 5). The 2-D and 3-D model results indicated that intracellular Ca^{2+} concentrations had no significant differences compared with the control (Fig. 6).

Discussion

In 1967, Reese and Karnovsky determined that tight junctions were not discontinuous and BBB existed based on the vascular endothelium. Historically, the BBB has been defined by the endothelial cell layer that forms the vessel/capillary walls. Recently, the concept of NVU was introduced to recognize that brain health involved functional interactions between neurons and non-neuronal cells (17). NVU plays a crucial role in brain maintenance via cellular interactions between microvessels and parenchyma. Non-neuronal cells are responsible for the CNS's physical, biochemical and immune barriers that regulate neuronal microenvironments, which is key for signal transduction, anginogenesis, and so forth (18).

Physiologically, NVU regulates cellular movements like vascular growth, nutrient supply, and brain protection. Adherens junctions (AJs) and tight junctions (TJs) as two key structures could reduce the paracellular flux across the brain endothelium, whereas transporters and receptors could carry some molecules that transfer large amino-acids and drugs to the brain. Brain homeostasis could be out of balance due to abnormal neuronal activity or toxicity by pathological stimuli (17).

Endothelial cell monolayer is commonly used as vitro models, but it only represents a simplified BBB model. This simplification does not consider the participation of other cell types, which are necessary for BBB maintenance (19,20). Later, co-culture model that involve astrocytes and endothelial cells are considered valid cell-based BBB model, as they contain TJs, transporters, and ionic channels. However, the absence of some cell types can decrease functional integrity (21). The tri-culture model was recently introduced which can be modified depending on research objectives using neurons or other cells as the third cell type (22, 23). The NVU model has become one of the most representative vitro models in studying human BBB regulation (24).

We chose Pb^{2+} and AL^{3+} as test materials due to their association with major global environmental health hazards. These chemicals can damage various body systems, such as the renal, hematopoietic, skeletal, and especially the central nervous system (25). Pb^{2+} produces a major toxic mechanism on calcium fluxes and calcium-regulated events (26,27,28). Other mechanisms affect oxidative stress, impacting membrane biophysics and changing cell signing. AL^{3+} produces a toxic mechanism that affects oxidative stress, membrane biologics, cell signaling, and neurotransmission (29,30-32,33).

Research from the mid-1990s has shown that astrocytes propagate intercellular Ca^{2+} waves over long distances in response to stimulation. Similar to neurons, astrocytes release transmitters in a Ca^{2+}-dependent manner. Moreover, astrocytes signal to neurons through Ca^{2+}-dependent glutamate release(34). Astrocytes are classically identified using histological analysis to test the intermediate filament glial fibrillary acidic proteins (GFAP) (35).

We cultured three cells in vitro, including astrocytes, BMECs, and the hippocampus. The cell viability declined for all three cell types as Pb^{2+} and Al^{3+} concentrations rose. The two models showed no significant differences compared with control group. In calculated intracellular Ca^{2+} concentrations, the results suggested that intracellular Ca^{2+} concentration increased with Pb^{2+} and Al^{3+} concentrations compared with control ($p<0.01$), while two models showed no significant differences compared with control ($p>0.05$).

Previous research showed Pb^{2+} and Al^{3+} mechanisms related to intracellular Ca^{2+}; our study showed that the intracellular Ca^{2+} of the two models had no significant changes compared with the control. Possible explanations for this phenomenon include their function as the BBB, or the treatment duration was not long enough. The intracellular Ca^{2+} change would also occur if treated with high concentrations for its stress response. Meanwhile, it may connect with an indirect reaction, which is related to signal pathways.

In this study, we successfully established two models in vitro to mimic the brain-blood barrier. These models can be used to study neurotoxic chemical mechanisms. They can also be applied for neurotoxicity screenings in drug tests. The NVU model is more integrated than the 2-D model and can better represent the BBB.
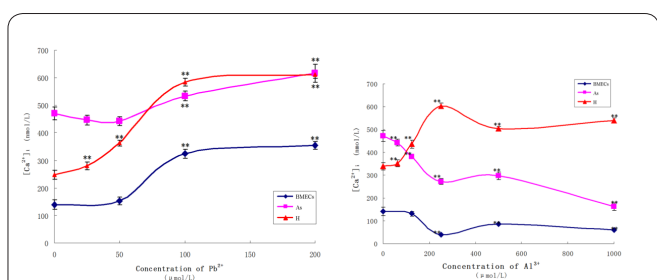
Figure 5. Intracellular Ca^{2+} concentrations of astrocytes, BMECs, and hippocampi treated with Pb^{2+} and Al^{3+}. The figures showed that intracellular Ca^{2+} concentrations increased with Pb^{2+} and Al^{3+} concentrations for all three cell types. ** represents P<0.01 compared with control group.
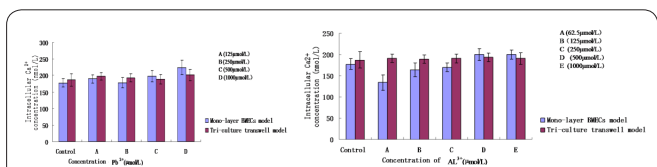
Figure 6. Intracellular Ca^{2+} concentration of mono-layer BMECs and Tri-culture Transwell treated with Pb^{2+} and Al^{3+}. There were no significant differences between the two models compared with control group (P>0.05).

References

1. Imola W, Csilla F, Istvan A. Krizbai. In vitro models of the blood-brain barrier. ActaNeurobiol Exp.2011; 71:113-28.

2. Hawkins BT, Davis TP. The blood-brain barrier/neurovascular unit in health and disease. Pharmacol.Rev. 2005; 57:173–85.

3. Abbott NJ, Patabendige AA, Dolman DE, Yusof SR, Begley DJ. Structure and function of the blood-brain barrier. Neurobiol Dis 2010;37: 13–25.

4. Abbott NJ, Friedman.A Overview and introduction: The blood-brain barrier in health and disease. Epilepsia 2012; 53(06):1-6.

5. Nakagawa S, Deli MA, Kawaguchi H, Shimizudani T, Shimono T, Kittel A, *et al*. A new blood-brain barrier model using primary rat brain endothelial cells,pericyts and astrocyte. NAEUROCHEM, Int. 2009;54:253-63

6. Hatherell, K, Couraud PO, Romero IA, Weksler B, Pilkington GJ. Development of a three-dimensional, all-human in vitro model of the blood-brain barrier using mono-, co-, and tri-cultivation Transwell models. J. NeurosciMehods2011;199:223-9.

7. Olson J, Holtzman D. Respiration and cell volume of primary cultured cerebral astrocytes in media of various osmolarities. Brain research1982;246: 273-9.

8. Diglio CA, Grammas P, Giacomelli F, Wiener J. Primary culture of rat cerebral microvascular endothelial cells. Isolation, growth, and characterization. Laboratory investigation, a journal of technical methods and pathology 1982; 46: 554-63.

9. Singer CA, Figueroa-Masot XA, Batchelor RH, DorsaDM.The mitogen-activated protein kinase pathway mediates estrogen neuro-protection after glutamate toxicity in primary cortical neurons. The Journal of neuroscience : the official journal of the Society for Neuroscience1999; 19: 2455-63

10. Schiera G, Sala S, Gallo A, Raffa MP, Pitarresi GL, Savettieri G, Di Liegro I. Permeability properties of a three-cell type in intro model of blood-brain barrier. J Cell Mol Med 2005;9:373-9.

11. Silva RF, Falcão AS, Fernandes A, Gordo AC, Brito MA, Brites D. Dissociated primary nerve cell cultures as models for assessment of neurotoxicity. Toxicol Lett 2006;163:1-9.

12. Gaillard PJ, de Boer AG.Relationship between permeability status of the blood-brain barrier and in vitro permeability coefficient of a drug. Eur J Pharm Sci 2000; 12:95-102.

13. Wilelm I, Fazakas C, KrizbaiIA.In vitro models of the blood-brain barrier. ActaNeurobiolExp2011;71:113-28.

14. Pardridge WM, Triguero D, Yang J, Cancilla PA .Comparison of in vitro and in vivo models of drug transcytosis through the blood-brain barrier. J. Pharmacol. Exp. Ther1990; 253:884-91.

15. Summerfield SG, Stevens AJ, Cutler L, del Carmen Osuna M, Hammond B, Tang SP, Hersey A, Spalding DJ, Jeffrey P.Improving the in vitro prediction of in vivo central nervous system penetration: integrating permeability, p-glycoprotein efflux, and free fractions in blood and brain. J.Phamacol. Exp. Ther2006; 316:1282-90.

16. Summerfield SG, Read K, Begley DJ, Obradovic T, Hidalgo IJ, Coggon S, Lewis AV, Porter RA, Jeffrey P. Central nervous system drug disposition: the relationship between in situ brain permeability and brain free fraction. J. Pharmacol. Exp. Ther.2007; 322:205-13.

17. Morin-Brureau,Morin-Brureau, Melanie, Frederic De Bock, and Mireille Lerner-Natoli. Organotypic brain slices a model to study the neurovascul and unit micro-environment in epilepsies. Fluids and Barriers CNS.2013;10(1):11.

18. Andrew D. Wong, Mao Ye, Amanda F. Levy. et al. The blood-brain barrier: an engineering perspective. Frontiers in Neuroengineering.2013; 6, 1-22.

19. Hamm S, Dehouck B, Kraus J, Wolburg-Buchholz K, Wolburg H, Risau W, Cecchelli R, Engelhardt B, Dehouck MP. Astrocytes mediated modulation of blood-brain barrier permeability dose not correlate with a loss of tight junction proteins from the cellular contacts. Cell Tissue Res 2004;315:157-66.

20. Hori S, Ohtsuki S, Tachikawa M, Kimura N, Kondo T, Watanabe M, Nakashima E, Terasaki T. Functional expression of rat ABCG2 on the luminal side of brain capillaries and its enhancement by astrocyte-derived soluble factor (s). J Neurochem2004; 90:526-36.

21. Dore-Duffy P, Cleary K. Morphology and properties of pericytes. Methods MolBiol2011; 686:49-68.

22. Cucullo L,Marchi N, Hossain M, Janigro D. A dynamic in vitro BBB model for the study of immune cell trafficking into the central nervous system. J Cereb Blood Flow 2011; 31:767-77.

23. Hallier-Vanuxeem D, Prieto P, Culot M, Diallo H, Landry C, Tähti H, Cecchelli R . New strategy for alerting central nervous system toxicity: integration of blood-brain barrier toxicity and permeability in neurotoxity assessment. Toxicol in vitro 2009;23:447-53.

24. Hatherell, K, Couraud, P.O., Romero, I.A., et al. Development of a three-dimensional, all-human in vitro model of the blood-brain barrier using mono-, co-, and tri-cultivation Transwell models. J. NeurosciMehods, 2011; 199:223-9.

25. Wilson MA, Johnston MV, Goldstein GW, Blue ME.Neonatal lead exposure impairs development of rodent barrel field cortex. Proc Natl AcadSci USA 2000; 97:5540-45.

26. Bressler J, Kim KA, Chakraborti T, Goldstein G. Molecular mechanisms of lead neurotoxicy, Neurochem Res 1999; 24:595-600.

27. Marchetti C. Molecular targets of lead in brain neurotoxicity, Neurotox RES 2003; 5:221-36.

28. Toscano CD, Guilarte TR. Lead neurotoxicity: from exposure to molecular effects. Brain Res Rev 2005; 49:529-54.

29. Sies H, Jone D. Oxidative Stress. In: Fink G (ed) Encyclopedia of stress. Elsevier, San Diego, 2007, pp. 45-48.

30. Kaneko N, Sugioka T, Sakurai H. Aluminum compounds enhance lipid peroxidation in liposomes: insight into cellular damage caused by oxidative stress. J InorgBiochem2007; 101:967-75.

31. Johnson VN, Kim SH, Sharma RP. Aluminum-maltolate induces apoptosis and necrosis in neuro-2a cells: potential role for p53 signaling. ToxicolSci2005; 83:329-39.

32. Mailloux RJ, Appanna VD. /Aluminum toxicity triggers the nuclear translocation of HIF-lalpha and promotes anaerobiosis in hepatocytes. ToxicolIn Vitro 2007; 21:16-24.

33. Corderio JM, Silva VS, Oliveira CR, Goncalves PP.Aluminium-induced impairment of Ca^{2+} modulatory action on GABA transport in brain cortex nerve terminals. J InorgBiochem2003; 97:132-42.

34. Fiacco TA, Agulhon C, McCarthy KD.Sorting out Astrocyte Physiology from Pharmacology. Annu. Rev. Pharmacol. Toxicol.2008; 49 (1): 151–74.

35. Venkatesh K, Srikanth L, Vengamma B, Chandrasekhar C, Sanjeevkumar A, Mouleshwara Prasad BC, Sarma PV. In vitro differentiation of cultured human CD34+ cells into astrocytes. Neurol India 2013; 61:383-8.